

Trains of magnetic holes and magnetic humps in the heliosheath

L. F. Burlaga,¹ N. F. Ness,² and M. H. Acuña³

Received 19 June 2006; revised 23 August 2006; accepted 1 September 2006; published 7 November 2006.

[1] This paper discusses the existence of trains (sequences) of magnetic holes and magnetic humps in the heliosheath, based on Voyager 1 observations made in the intervals DOY 312.9707–317.0879, 2005 and DOY 185.2762–186.7957, 2005. These two trains represent a class of compressive fluctuations in the heliosheath. Varying from one region or time interval to another, this class of fluctuations probably depends on the varying conditions upstream of the Termination Shock and its nature. The trains of magnetic holes in the heliosheath resemble certain magnetic field strength fluctuations observed in planetary magnetosheaths. **Citation:** Burlaga, L. F., N. F. Ness, and M. H. Acuña (2006), Trains of magnetic holes and magnetic humps in the heliosheath, *Geophys. Res. Lett.*, 33, L21106, doi:10.1029/2006GL027276.

1. Introduction

[2] Voyager 1 (V1) crossed the termination shock on \approx DOY 350, 2004 [Stone *et al.*, 2005; Gurnett and Kurth, 2005; Decker *et al.*, 2005; Burlaga *et al.*, 2005], and it has been moving through the heliosheath since that time. Burlaga *et al.* [2006] studied magnetic field fluctuations within a sector that passed V1 from DOY 360, 2005 to DOY 110, 2006. The fluctuations in the magnetic field strength B were the dominant feature, but there was also a significant component of fluctuations in the direction transverse to $\langle \mathbf{B} \rangle$. These compressive variations in the heliosheath are unlike the nearly non-compressive variations observed in the supersonic solar wind and studied extensively [Burlaga, 1995].

[3] This paper demonstrates the existence of sequences or trains of magnetic holes and magnetic humps in the heliosheath (Sections 2 and 3), using observations from the magnetic field experiment on Voyager 1. We discuss two trains observed on DOY 312–317 (“interval-1”, containing primarily magnetic holes) and DOY 185/186, 2005 (“interval-2”, containing primarily magnetic humps). These are the most extended and dramatic sets of magnetic holes and magnetic humps observed in the heliosheath from the time of the termination shock crossing on DOY 350, 2004 to the latest available data on DOY 317, 2005, but relatively isolated magnetic holes and humps have been observed throughout the heliosheath in this interval. It is likely V1 was significantly farther from the termination shock (TS) in these two intervals than in the interval discussed by Burlaga

et al. [2006], since the TS was most likely moving toward the sun at the time it was crossed [Whang *et al.*, 2004; Jokipii, 2005].

[4] The highly compressive fluctuations in \mathbf{B} that we shall discuss resemble the fluctuations in \mathbf{B} observed in certain regions of planetary magnetosheaths. They were observed in the magnetosheaths of Jupiter [Erdős and Balogh, 1996], Saturn [Bavassano Cattaneo *et al.*, 1998] and Earth [e.g., see McKean *et al.*, 1992]. The relationship between the highly compressive fluctuations in the heliosheath and the so-called “mirror structures” in planetary magnetosheaths is discussed in Section 4.

2. A Train of Magnetic Holes

[5] A “train of magnetic holes” (including a few magnetic humps and variations that cannot be clearly identified as magnetic holes or humps) was observed in the heliosheath by V1 for more than 4 days from DOY 312.97067 to 317.08789, 2005 (interval-2). The terminology (also used in the subject of planetary magnetosheaths) is a suggestive and useful but oversimplified way of describing the elements of the complex signal in Figure 1. The observations of 48 sec averages of the magnetic field strength B , azimuthal angle λ , and elevation angle δ are shown in Figures 1a, 1b, and 1c, respectively. A distribution of B , which is not included, shows two peaks: 1) a narrow peak at relatively high fields, corresponding to an upper ‘baseline’ near 0.3 nT and 2) a broader peak at lower fields corresponding to “magnetic holes”. The average magnetic field strength is $\langle B \rangle = 0.23$ nT and the standard deviation is $SD = 0.07$, giving $2 \times SD / \langle B \rangle = 0.64$, which shows that the fluctuations in B are nonlinear. Figure 1 shows that the direction of \mathbf{B} is relatively constant and the fluctuations in the direction of \mathbf{B} are relatively small in the interval-1. The standard deviations of λ and δ are 9.8° and 24° , respectively. The fluctuations in δ are small but not negligible, and they appear to be related to changes in B . The average magnetic field direction is given by $\langle \lambda \rangle = 23.5^\circ \pm 0.4^\circ$ and $\langle \delta \rangle = 9.8^\circ \pm 0.2^\circ$, where the uncertainties are the standard errors in the mean. The magnetic field in this interval is directed nearly along the sun-S/C line, if systematic errors are negligible. In general, the uncertainty in each of the components is approximately ± 0.015 nT on average, largely due to systematic errors; the systematic errors are actually variable, but they cannot be determined precisely for any given day.

[6] Magnetic holes and magnetic humps were identified in the solar wind at 1 AU by Turner *et al.* [1977] as isolated depressions and enhancements in the magnetic field with a characteristic size of the order of 20 gyroradii, (R_L) for thermal protons in the supersonic solar wind. An example of an isolated magnetic hole in the heliosheath was discussed in detail by Burlaga *et al.* [2006]; its magnetic field strength profile is shown in Figure 2a. The smooth curve in the

¹Geospace Physics Laboratory, NASA Goddard Space Flight Center, Greenbelt, Maryland, USA.

²Institute for Astrophysics and Computational Sciences, Catholic University of America, Washington, D. C., USA.

³Planetary Magnetospheres Laboratory, NASA Goddard Space Flight Center, Greenbelt, Maryland, USA.

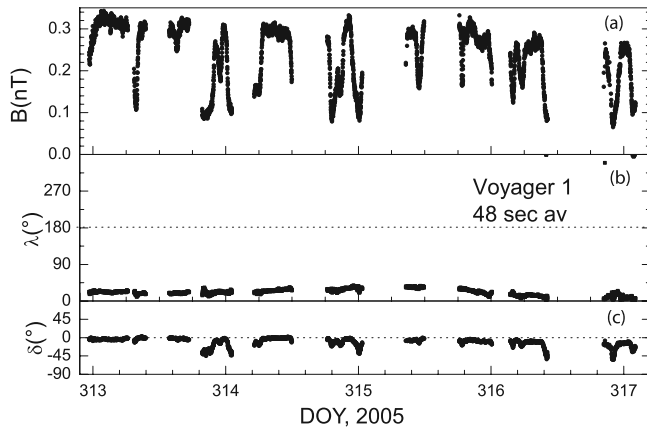


Figure 1. Forty-eight second averages of (top) magnetic field strength, (middle) azimuthal angle, and (bottom) elevation angle of the magnetic field in the heliosheath from DOY 313–317, 2005. A train of highly compressive magnetic field fluctuations, mainly magnetic holes, is observed, with relatively little change in the magnetic field direction.

Figure 2a is a Gaussian fit to the data, which provides a good description of the shape of the magnetic hole, and gives a ratio of $B_o/B_{\min} = 4.4$. Assuming that the convective speed of the parcel of plasma was ≈ 20 km/sec, a passage time of ≈ 125 min, corresponds to $\approx 10 R_L \approx 150,000$ km = $0(0.001$ AU) [see *Burlaga et al.*, 2006].

[7] Magnetic humps [Turner et al., 1977] are similar to magnetic holes in size and profile except that the field strength increases. An example of an isolated magnetic hump in the heliosheath observed by V1 on DOY 246, 2005 is shown in Figure 2b. The direction of the magnetic field was constant across this magnetic hump. The curve in Figure 2b is a Gaussian fit to the data, which provides a very good description of the shape, gives a ratio $B_{\max}/B_o = 2.7$, and gives a passage time of ≈ 180 min, comparable to that of the magnetic hole in Figure 2a.

[8] The feature at the end of DOY 304 in Figure 1a can be modeled as a superposition of three magnetic holes with Gaussian profiles, shown by the solid curve in Figure 2c. This suggests that three magnetic holes grew and merged either by the broadening of non-propagating structures or by the interaction of propagating structures. The feature at the end of DOY 313 in Figure 1a can be described as the superposition of two magnetic humps, as shown by the fit with two Gaussian distributions, suggesting that two neighboring magnetic humps merged as they grew.

[9] The sizes of the magnetic holes and magnetic humps in interval-1 are related to the time intervals associated with their motion past V1. A magnetic hole (magnetic hump) is characterized by a short time interval in which there is a large decrease (increase) in B followed by a similar interval with a large increase (decrease) in B . There are several data gaps, owing to a lack of continuous data when there is no tracking of the spacecraft telemetry signal. There are isolated decreases and increases in B that might be related to magnetic holes and humps that were truncated by data gaps. In Figure 1a the passage times of 22 intervals in which there was either a large increase or decrease in B range from ≈ 1

to ≈ 110 minutes, with a mean of 56 ± 5 min and a standard deviation of 23 min. We assume that the structures are convected past V1 and that their propagation speed relative to the ambient plasma is either zero or small compared to the convection speed. The convection speed in the interval DOY 313–317 was 81 ± 4 km/s (R. B. Decker, personal communication). Thus, the characteristic size of an increase or decrease in B is of the order of $L \approx 270,000$ km and the SD is $\approx 110,000$ km. The apparent size of the magnetic holes along the radial direction is $\approx 2 L \approx 540,000$ km. The size of magnetic holes in the heliosheath is much larger than the size of kinetic magnetic holes in the solar wind. For a characteristic pickup proton gyroradius of $\approx 15,000$ km in the heliosheath [Decker et al., 2005] the size of magnetic holes in the heliosheath is $\approx 35 R_L$, of the same order as that in the solar wind.

[10] A minimum variance analysis of the 48 sec averages of the components of the magnetic field in interval-1 gives the eigenvalues 0.0002, 0.0008, and 0.0059 (with the ratio of intermediate to minimum variance being 4 and the ratio of maximum to minimum variance being 7). Thus, the minimum variance direction is $\lambda_m \approx (-0.017, -0.284, 0.959)$ and maximum variance direction ($\lambda_M \approx -0.881, -0.450, -0.149$) (in RTN coordinates). In general, the eigenvalue ratio is not sufficient to determine the uncertainty in λ_m and λ_M , [see, e.g., Knetter et al., 2004], so the numbers above are only rough estimates. The variation of \mathbf{B} is primarily in the plane defined by λ_M and the intermediate variance direction $\lambda_i = (-0.473, 0.848, 0.243)$. The average magnetic field strength is $\langle B \rangle = 0.239$ nT, and the average component of the magnetic field in the maximum variance direction is 0.225 nT, very close to $\langle B \rangle$, consistent with

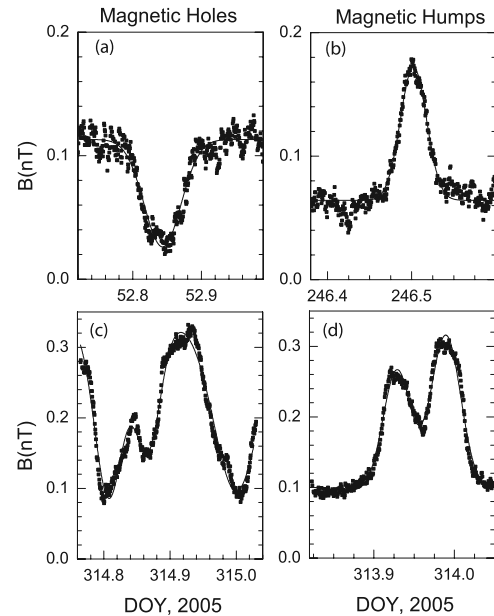


Figure 2. Forty-eight second averages of the magnetic field strength. (top left) An isolated magnetic hole, and a Gaussian fit shown by the curve. (top right) An isolated magnetic hump, and a Gaussian fit. (bottom left) A superposition of 3 magnetic holes, and a fit to three Gaussian functions. (bottom right) A superposition of 2 magnetic humps, and a fit to two Gaussian functions.

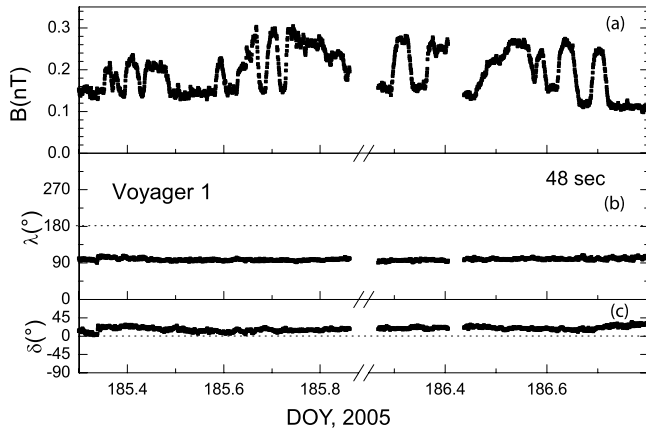


Figure 3. Forty-eight second averages of (top) magnetic field strength, (middle) azimuthal angle, and (bottom) elevation angle of the magnetic field in the heliosheath from DOY 313–317, 2005. A train of highly compressive magnetic field fluctuations, mainly magnetic humps, is observed, with essentially no change in the magnetic field direction.

highly compressive fluctuations. The strength of average magnetic field in the intermediate variance direction is $B_i = -0.035$ nT. The angle between \mathbf{B} and the maximum variance direction is $\theta_M = \cos^{-1}(B_M/B) = 17^\circ$. The angle between \mathbf{B} and the minimum variance direction is $\theta_m = \cos^{-1}(B_m/B) = 75^\circ$. A large value of θ_m is necessary for the growth of the mirror instability (See Section 4).

3. A Train of Magnetic Humps

[11] Highly compressive fluctuations in the heliosheath that appear to be a mainly a “train or sequence of magnetic humps” are shown in Figure 3. The terminology is a suggestive and useful but oversimplified way of describing the elements of the complex signal in Figure 3. The format is the same as that in Figure 1, and again the points are 48 sec averages. A distribution of B , (which is not included because of page limitations) shows two peaks: 1) a narrow peak corresponding to a low ‘baseline’ near 0.15 nT and 2) a broader peak of stronger fields corresponding to “magnetic humps”. The fluctuations were observed by V1 during at least two days, from DOY 185.2762 to 186.7957, 2005 (interval-2). This interval is closer to the time of TS crossing than interval-1, suggesting that the fluctuations in Figure 3 are closer to the TS and therefore less evolved than those in Figure 1. However, the distance to the termination shock cannot be determined, because the motion of the TS is not measured.

[12] The average magnetic field strength in Figure 3a is $\langle B \rangle = 0.192 \pm 0.001$ nT and the standard deviation is $SD = 0.053$ nT, giving $2 \times SD/\langle B \rangle = 0.55$ as a measure of the amplitude of the nonlinear fluctuations in B . Inspection of Figures 3b and 3c shows that the direction of \mathbf{B} is remarkably constant in interval-2. The standard deviations of λ and δ are only 3.0° and 5.0° , respectively. The average magnetic field directions is given by $\langle \lambda \rangle = 98.7^\circ \pm 0.1^\circ$ and $\langle \delta \rangle = 18.0^\circ \pm 0.1^\circ$, where the uncertainty for each is the standard error in the mean. The magnetic field in this interval is

nearly transverse to the sun-S/C line, assuming that systematic errors are negligible.

[13] The size of the regions in which large-scale decreases and increase in B occur (primarily at magnetic humps and in broader regions bounded by such changes) can be estimated from the passage times. The passage times of 23 large gradients in B in Figure 3a range from ≈ 9 to ≈ 43 minutes, with a mean of 21 ± 2 min and a standard deviation of 7 min. The average passage time of the increases (21 min) is approximately the same as that of the decreases (25 min), suggesting an apparent symmetry. The convection speed in the interval DOY 185–186 was 70 ± 5 km/s (R. B. Decker, personal communication). Thus, the characteristic size of an increase or decrease in B is of the order of $L \approx 90,000$ km and the SD is $\approx 30,000$ km. The size of the magnetic holes along the radial direction is $\approx 2 L \approx 180,000$ km. This is somewhat smaller than the size of the magnetic holes discussed in Section 2, but it could reflect different ambient conditions in region-1 and region-2, or a growth of the structure with increasing distance from the termination shock, rather than different physical structure.

[14] A minimum variance analysis of the 48 sec averages of the components of the magnetic field in interval-2 gives the eigenvalues 0.0001, 0.0002, and 0.0028, indicating nearly linear polarization along the maximum variance direction $\lambda_M = (-0.097, 0.9634, 0.250)$ in RTN coordinates. The minimum variance direction is $\lambda_m = (0.961, 0.025, 0.276)$, and the intermediate variance direction is $\lambda_i = (0.260, 0.267, -0.928)$. The average magnetic field strength is $\langle B \rangle = 0.192$ nT, and the average magnetic field strength in the maximum variance direction is 0.191 nT, very close to $\langle B \rangle$ consistent with highly compressive fluctuations. The angle between \mathbf{B} and the maximum variance direction is $\theta_M = \cos^{-1}(B_M/B) = 4^\circ$. The angle between \mathbf{B} and the minimum variance direction is $\theta_m = \cos^{-1}(B_m/B) = 88.5^\circ$.

4. Summary and Discussion

[15] We have discussed the V1 observations of the existence of trains of highly compressive fluctuations of the magnetic field in the heliosheath. A train observed on DOY 185/186, 2005 appears to be primarily a series of magnetic humps. A second train, observed from \approx DOY 312–318, 2005, appears to be primarily a series of magnetic holes.

[16] *Burlaga et al.* [2006] analyzed an interval containing compressive turbulence with significant fluctuations in all three components of the magnetic field. It is clear that the “turbulence” in the heliosheath is more complex than an extrapolation of these earlier observations would suggest. The magnetic “turbulence” in the heliosheath is very compressive (unlike the supersonic solar wind), but the nature of the compressive fluctuations varies depending on the time and the region examined.

[17] The nature and origin(s) of the compressive fluctuations in the heliosheath are not fully understood. The trains of magnetic holes and magnetic humps in the heliosheath are similar in some respects to the fluctuations often observed in planetary magnetosheaths.

[18] Many authors suggested that the mirror mode instability [*Hasegawa*, 1969] can cause fluctuations in B in planetary magnetosheaths [*McKean et al.*, 1992; *Erdős and*

Balogh, 1996] and in the isolated magnetic holes in the solar wind [Tsurutani *et al.*, 1992]. The mirror mode instability grows in a high β plasma when $T_{\perp}/T_{\parallel} > 1 + 1/\beta_{\perp}$ (the subscripts refer to perpendicular and parallel to the magnetic field) and saturates when $T_{\perp}/T_{\parallel} = 1 + 1/\beta_{\perp}$. The mirror instability implies the existence of an anisotropy $T_{\perp}/T_{\parallel} \geq 1$. Such an anisotropy has not been seen in the preliminary data from the lowest (40–53 KeV energy channel of the LECP experiment on V1, but an upper limit on T_{\perp}/T_{\parallel} has not yet been determined (R. B. Decker, personal communication).

[19] Another hypothesis is that magnetic holes and magnetic humps are MHD solitons [Baumgärtel, 1999]. Observations from CLUSTER support this view [Staciewicz, 2003]. However, the size of magnetic holes and humps is of the order of 20 gyroradii, where fluid theories (including Hall MHD models) break down for high β plasmas [Schwartz *et al.*, 1996].

[20] Burlaga and Lemaire [1978] showed that magnetic holes and humps can be modeled as pressure balanced structures which are static solutions of the Vlasov-Maxwell equations for a slab geometry. The Vlasov/Maxwell equations are the appropriate equations for describing magnetic holes and humps [Schwartz *et al.*, 1996], but they are difficult to solve in general.

[21] A hybrid code can describe the growth and decay or saturation of magnetic holes and humps [Baumgärtel *et al.*, 2005]. This type of model does not produce the propagating soliton structures, but it does account for a non-propagating pressure balanced structure with \mathbf{k} nearly perpendicular to \mathbf{B} . Baumgärtel *et al.* [2003] showed that a magnetic hole that initially has a Gaussian profile for B but no pressure balance evolves to a pressure-balanced structure, maintaining a Gaussian profile for B .

[22] One can consider the hypothesis that the termination shock, which tends to be a perpendicular shock on average where V1 crossed it, often generates a large temperature anisotropy with $T_{\perp}/T_{\parallel} > 1$. It is thought that β is high in the heliosheath, both because the medium is heated by the TS and because the protons that dominate the temperature are energetic protons (possibly shock accelerated particles and/or pickup protons that are compressed and heated by the TS). Thus, the mirror instability might occur at times in the heliosheath and produce magnetic humps and magnetic holes that evolve with time in various ways depending on ambient conditions. Eventually the mirror instability reduces the temperature anisotropy until growth of the structures stops.

[23] **Acknowledgments.** N. F. Ness was partially supported by grant NNG05GK25G to the Catholic University of America. T. McClanahan and S. Kramer processed the data, and R. Fernandez-Borda computed the “zero-tables” that were used in the data processing. We thank R. Decker and the Principal Investigator (T. Krimigis) of the LECP experiment for

providing the speeds of the plasma for the two intervals considered and for searching for anisotropies in the particle distributions. One of us (L. B.) thanks K. Baumgärtel for very helpful comments.

References

- Baumgärtel, K. (1999), Soliton approach to magnetic holes, *J. Geophys. Res.*, *104*, 28,295–28,308.
- Baumgärtel, K., K. Sauer, and E. Dubinin (2003), Towards understanding magnetic holes: Hybrid simulations, *Geophys. Res. Lett.*, *30*(14), 1761, doi:10.1029/2003GL017373.
- Baumgärtel, K., K. Sauer, and E. Dubinin (2005), Kinetic slow mode-type solitons, *Nonlinear Processes Geophys.*, *12*, 291–298.
- Bavassano Cattaneo, M. B., C. Basile, G. Moreno, and J. D. Richardson (1998), Evolution of mirror structures in the magnetosheath of Saturn from the bow shock to the magnetopause, *J. Geophys. Res.*, *103*, 11,961–11,972.
- Burlaga, L. F. (1995), *Interplanetary Magnetohydrodynamics*, Oxford Univ. Press, New York.
- Burlaga, L. F., and J. F. Lemaire (1978), Interplanetary magnetic holes: Theory, *J. Geophys. Res.*, *83*, 5157–5160.
- Burlaga, L. F., N. F. Ness, M. H. Acuña, R. P. Lepping, J. E. P. Connerney, E. C. Stone, and F. B. McDonald (2005), Crossing the termination shock into the heliosheath: Magnetic fields, *Science*, *309*, 2027–2029.
- Burlaga, L. F., N. F. Ness, and M. H. Acuña (2006), Magnetic fields in the heliosheath: Voyager 1 observations, *Astrophys. J.*, *642*, 584–592.
- Decker, R. B., S. M. Krimigis, E. C. Roelof, M. E. Hill, T. P. Armstrong, G. Gloeckler, D. C. Hamilton, and L. J. Lanzerotti (2005), Voyager 1 in the foreshock, termination shock, and heliosheath, *Science*, *309*, 2020–2024.
- Erdős, G., and A. Balogh (1996), Statistical properties of mirror mode structures observed by Ulysses in the magnetosheath of Jupiter, *J. Geophys. Res.*, *101*, 1–12.
- Gurnett, D. A., and W. S. Kurth (2005), Electron plasma oscillations upstream of the solar wind termination shock, *Science*, *309*, 2025–2027.
- Hasegawa, A. (1969), Drift mirror instability in the magnetosphere, *Phys. Fluids*, *12*, 2642.
- Jokipii, J. R. (2005), The magnetic field structure in the heliosheath, *Ap. J.*, *631*, L163–L165.
- Knetter, T., F. M. Neubauer, T. Horbury, and A. Balogh (2004), Four-point discontinuity observations using Cluster magnetic field data: A statistical survey, *J. Geophys. Res.*, *109*, A06102, doi:10.1029/2003JA010099.
- McKean, M. E., D. Winske, and S. P. Gary (1992), Mirror and ion cyclotron anisotropy instabilities in the magnetosheath, *J. Geophys. Res.*, *97*, 19,421–19,432.
- Schwartz, S., D. Burgess, and J. J. Moses (1996), Low frequency waves in the Earth’s magnetosheath: Present status, *Ann. Geophys.*, *14*, 1123–1150.
- Staciewicz, K. (2003), Theory and observations of slow-mode solitons in space plasmas, *Phys. Rev. Lett.*, *93*(12), 125004.
- Stone, E. C., A. C. Cummings, F. B. McDonald, B. C. Heikkila, N. Lal, and W. R. Webber (2005), Voyager 1 explores the termination shock region and the heliosheath beyond September 2005, *Science*, *309*, 2017–2020.
- Tsurutani, B. T., D. Southwood, E. J. Smith, and A. Balogh (1992), Non-linear magnetosonic waves and mirror mode structures in the March 1991 Ulysses interplanetary event, *Geophys. Res. Lett.*, *19*, 1267–1270.
- Turner, J. M., L. F. Burlaga, N. F. Ness, and J. F. Lemaire (1977), Magnetic holes in the solar wind, *J. Geophys. Res.*, *82*, 1921–1924.
- Whang, Y. C., L. F. Burlaga, Y. M. Wang, and N. R. Sheeley (2004), The termination shock near 35 degrees latitude, *Geophys. Res. Lett.*, *31*, L03805, doi:10.1029/2003GL018679.

M. H. Acuña, Planetary Magnetospheres Laboratory, Code 695, NASA/Goddard Space Flight Center, Greenbelt, MD 20771, USA.

L. F. Burlaga, Geospace Physics Laboratory, Code 673, NASA Goddard Space Flight Center, Greenbelt, MD 20771, USA. (leonard.f.burlaga@nasa.gov)

N. F. Ness, Institute for Astrophysics and Computational Sciences, Catholic University of America, Washington, D. C. 20064, USA.